ACS Catalysis

Research Article

pubs.acs.org/acscatalysis

MgO- and Pt-Promoted TiO_2 as an Efficient Photocatalyst for the Preferential Reduction of Carbon Dioxide in the Presence of Water

Shunji Xie, Yu Wang, Qinghong Zhang,* Weiping Deng, and Ye Wang*

State Key Laboratory of Physical Chemistry of Solid Surfaces, Collaborative Innovation Center of Chemistry for Energy Materials, National Engineering Laboratory for Green Chemical Productions of Alcohols, Ethers and Esters, College of Chemistry and Chemical Engineering, Xiamen University, Xiamen 361005, China

ABSTRACT: The photocatalytic reduction of carbon dioxide with water to fuels and chemicals is a longstanding challenge. This article focuses on the effects of cocatalysts and reaction modes on photocatalytic behaviors of TiO_2 with an emphasis on the selectivity of photogenerated electrons for CO_2 reduction in the presence of H_2O, which has been overlooked in most of the published papers. Our results clarified that the reaction using H_2O vapor exhibited significantly higher selectivity for CO_2 reduction than that by immersing the photocatalyst into liquid H_2O. We examined the effect of noble metal cocatalysts and found that the rate of CH_4 formation increased in the sequence of Ag < Rh < Au < Pd < Pt, corresponding well to the increase in the efficiency of electron−hole separation. This indicates that Pt is the most effective cocatalyst to extract photogenerated electrons for CO_2 reduction. The selectivity of CH_4 in CO_2 reduction was also enhanced by Pt. The size and loading amount of Pt affected the activity; a smaller mean size of Pt particles and an appropriate loading amount favored the formation of reduction products. The reduction of H_2O to H_2 was accelerated more than the reduction of CO_2 in the presence of Pt, leading to a lower selectivity for CO_2 reduction and limited increases in CH_4 formation rate. We demonstrated that the addition of MgO into the Pt−TiO_2 catalyst could further enhance the formation of CH_4. The formation of H_2 was suppressed simultaneously, suggesting the increase in the selectivity for CO_2 reduction in the presence of MgO. Furthermore, the MgO- and Pt-modified TiO_2 catalyst exhibited a higher CH_4 selectivity in CO_2 reduction.

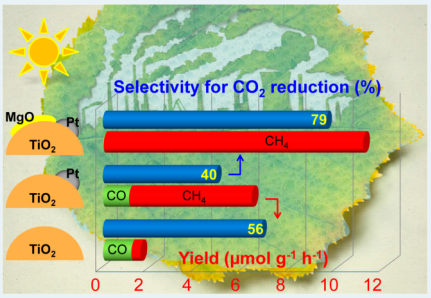

KEYWORDS: *photocatalysis, carbon dioxide, preferential reduction, methane, titanium oxide, cocatalyst*

1. INTRODUCTION

Carbon dioxide is widely accepted as a major greenhouse gas which causes global environmental problems. The concerns on the emissions of CO_2 have been growing rapidly. On the other hand, the diminishing of fossil resources, in particular petroleum, has driven research activities toward finding other carbon resources for the production of fuels and chemicals. Under these backgrounds, the capture and utilization of CO_2 as an alternative carbon feedstock have attracted much research attention in recent years.[1] It is highly desirable to establish a carbon-neutral cycle by transformation of CO_2 produced in the energy and chemical industries into fuels and chemicals. However, the activation and conversion of CO_2 is a big challenge because CO_2 is one of the most stable small molecules. The dissociation energy of C═O bond in CO_2 is ~750 kJ mol^{-1}, higher than those of many other chemical bonds such as C−H (~430 kJ mol^{-1}) and C−C (~336 kJ mol^{-1}). There are two main routes for the conversion of CO_2: (1) cofeeding a high-energy reactant such as H_2, unsaturated compound, epoxide, or organometallic compound with CO_2; (2) supplying external energy such as solar or electric energy.[1]

In nature, the photosynthesis of green plants transforms CO_2 in the presence of H_2O with sunlight into carbohydrates and O_2 owing to the catalytic function of chlorophyll. Inspired by this nature system, many research groups attempt to use artificial photosynthesis for the reduction of CO_2 with H_2O to chemicals or fuels. Inoue et al. reported a pioneering work for the photocatalytic reduction of CO_2 in H_2O in 1979.[2] They found that several semiconductors such as SiC, GaP, and TiO_2 suspended in water could catalyze the photoreduction of CO_2, forming organic compounds. Since then, many studies have been devoted to the semiconductor-based photocatalytic reduction of CO_2 with H_2O and the pace has increased enormously in recent years.[3−13] Various semiconductors such as TiO_2,[14,15] Ga_2O_3,[16,17] $ZnGe_2O_4$,[18,19] $ZnGa_2O_4$,[20,21] Ba-$La_4Ti_4O_{15}$,[22] $W_{18}O_{49}$ nanowires,[23] WO_3 nanosheets,[24] and nanostructured Bi_2WO_6[25−27] have been reported to be efficient catalysts for the photocatalytic reduction of CO_2. Although some progress has been made in this area, the photocatalytic activity for CO_2 reduction is still quite low.

Some challenges such as poor light-harvesting capacity and low quantum efficiency because of the rapid recombination of photogenerated electrons and holes are known for photocatalysis. In addition to these common challenges, the low adsorption ability of CO_2 on catalyst surfaces and the low activity of the catalyst surface toward CO_2 activation further

Received: May 12, 2014
Revised: August 12, 2014
Published: September 5, 2014

increase the difficulty in the photocatalytic reduction of CO_2. Moreover, the reduction of H_2O by the photogenerated electrons into H_2 would also proceed over the photocatalyst and thus may be a competitive reaction with the photocatalytic reduction of CO_2.

Several strategies such as the preparation of semiconductors with different crystalline structures or morphologies, the addition of noble or coinage metals onto the semiconductor, and the preparation of semiconductor-based nanocomposites have been proposed to increase the photocatalytic activity for CO_2 reduction.[14,15,28−34] However, most of these strategies have also been reported to be capable of enhancing the photocatalytic reduction of H_2O to H_2. Only few studies have been devoted to developing strategies to increase the selectivity of photogenerated electrons for CO_2 reduction. Recently, we found that the design and preparation of a Pt@Cu_2O core−shell structured cocatalyst on TiO_2 could significantly promote the reduction of CO_2 to CH_4 and suppress the reduction of H_2O to H_2.[35] Although many studies have reported the enhancement of CO_2 reduction by cocatalysts, the information on the effect of cocatalysts on the selectivity of photogenerated electrons used for CO_2 reduction is very limited.

Moreover, different reaction modes have been employed for the photocatalytic reduction of CO_2 with H_2O. Typically, the photocatalyst is either immersed into the aqueous solution, where CO_2 is dissolved and the solid−liquid interface photoreaction occurs, or placed on a catalyst holder surrounded by CO_2 and H_2O vapor, where the solid−gas interface photoreaction takes place.[9] The former reaction mode has been adopted in a lot of research, but limitations such as the lower solubility of CO_2 in H_2O, the preferential adsorption of H_2O on catalyst surfaces, and the difficult separation of a small amount of products from H_2O can be expected.[10] To increase the solubility of CO_2 in liquid phase, an alkaline medium is usually employed.[9,10] However, the formed CO_3^{2-} or HCO_3^- is typically more difficult to reduce than CO_2, and CO_3^{2-} is known as a good hole quencher.[10] Therefore, the solid−gas interface reaction mode using H_2O vapor seems more attractive.[9,10] However, to the best of our knowledge, thus far, there has been no direct comparison of the photocatalytic behaviors using the two reaction modes for the same catalytic system.

In this paper, we first investigate the influence of the reaction mode (solid−liquid or solid−gas) on the photocatalytic behaviors of TiO_2 and Pt-promoted TiO_2. Then, we focus on studying the effect of cocatalysts of TiO_2 for photocatalytic reduction of CO_2 to CH_4 and CO using the solid−gas interface reaction mode. We also pay attention to the effect of cocatalysts on the reduction of H_2O to H_2 and the selectivity of photogenerated electrons used for CO_2 reduction. The present paper attempts to provide insights for the design of photocatalytic systems capable of performing preferential reduction of CO_2 in the presence of H_2O.

2. EXPERIMENTAL SECTION

2.1. Catalyst Preparation. TiO_2 (P25), which contained 20% rutile and 80% anatase, was purchased from Degussa. The noble metal-promoted TiO_2 (denoted as M−TiO_2, and M = Pt, Pd, Au, Rh, or Ag) catalysts were typically prepared by a photodeposition method. For example, for the preparation of Pt−TiO_2, a fixed amount of TiO_2 was suspended in an aqueous solution of hexachloroplatinic acid (H_2PtCl_6) containing 0.1 M methanol as a hole scavenger. The suspension was irradiated with a 300 W Hg lamp for 2 h. The obtained sample was recovered by filtration, followed by washing repeatedly with deionized water and drying at 373 K for 12 h. The impregnation followed by H_2 reduction and the chemical reduction with hydrazine were also employed for the preparation of Pt-promoted TiO_2 photocatalysts for comparison, and the catalysts were denoted as Pt−TiO_2−*imp*−H_2 and Pt−TiO_2−*hydrazine*, respectively. For the impregnation, a fixed amount of TiO_2 was suspended in an aqueous solution of H_2PtCl_6. Then, water was evaporated, and the recovered solid sample was further dried. Finally, the sample was reduced in H_2 gas flow at 623 K for 2 h. For the chemical reduction with hydrazine, an aqueous solution of hydrazine was added dropwise into the suspension containing powdery TiO_2 in the aqueous solution of H_2PtCl_6. After the reduction, the sample was recovered by filtration, followed by washing thoroughly with deionized water and drying overnight. MgO-modified TiO_2 samples were prepared with an impregnation method by immersing powdery TiO_2 into an aqueous solution of $Mg(NO_3)_2$. After impregnation and drying, the sample was calcined in air at 773 K for 4 h. The MgO- and Pt-doubly modified TiO_2 (denoted as MgO−Pt−TiO_2) catalysts were prepared by the photodeposition of Pt onto the MgO-modified TiO_2 sample using the same procedure as that for the preparation of Pt−TiO_2.

2.2. Characterization. The photocatalysts were characterized by a series of techniques including powder X-ray diffraction (XRD), transmission electron microscopy (TEM), photoluminescence (PL) spectroscopy, CO_2 chemisorption, and photoelectrochemical measurements. The XRD patterns were collected on a Panalytical X'pert Pro diffractometer using Cu Kα radiation (40 kV, 30 mA). The TEM measurements were performed on a JEM-2100 electron microscope operated at an acceleration voltage of 200 kV. The PL spectra were obtained on an Edinburgh Analytical Instrument FLS 920 spectrophotometer with an excitation wavelength of 365 nm. The amount of CO_2 chemisorption was measured at 298 K with a Micromeritics ASAP2020C apparatus by adopting the procedure reported by Teramura et al.[36] The photoelectrochemical measurements were carried out with an Ivium CompactStat (Holland) using a standard three-electrode cell with a working electrode, a Pt wire as the counter electrode, and an SCE electrode as the reference electrode.[37] A 0.5 M Na_2SO_4 aqueous solution was used as the electrolyte. The working electrode was prepared by cleaning an F-doped SnO_2-coated glass (FTO glass, 1 cm × 2 cm). The photocatalyst was dispersed in ethanol, and the suspension was added dropwise directly onto the FTO by microsyringe with a gentle stream of air to speed drying. The film was dried at 393 K for 1 h, and the typical surface density of the photocatalyst was 1 mg cm^{-2}.

2.3. Catalytic Reaction. The photocatalytic reduction of CO_2 with H_2O was carried out in a stainless-steel reactor (volume, ∼100 mL) with a quartz window on the top of the reactor. The light source was 100 W Xe lamp (Beijing Trusttech Co., Ltd.) at UV−vis (λ = 320−780 nm). The light intensities measured by an optical power meter (Beijing Aulight Co., Ltd., CEL-NP2000−10) were 580 and 60 mW cm^{-2} in the ranges of 320−780 and 320−400 nm, respectively, and the fraction of the UV light in the spectrum was approximately 10%. For the solid−gas interface reaction mode, 20 mg of solid catalyst was placed on a Teflon catalyst holder in the upper region of the reactor (Figure 1, left). Liquid water with a volume of 4.0 mL was precharged in the bottom of the reactor.

dx.doi.org/10.1021/cs500648p | ACS Catal. 2014, 4, 3644−3653

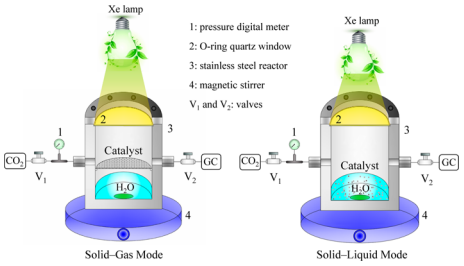

Figure 1. Reactor used for photocatalytic reduction of CO_2 with H_2O. Left: solid−gas mode, right: solid−liquid mode. The distance between the Xe lamp and the catalyst was adjusted to be the same for the two reaction modes.

The catalyst was surrounded by CO_2 and H_2O vapor. The pressure of CO_2 was typically regulated to 0.2 MPa. The temperature of the reactor was kept at 323 K, and the vapor pressure of H_2O was 12.3 kPa under such a circumstance. For the solid−liquid interface reaction mode (Figure 1, right), the catalyst was dispersed in 4.0 mL water, which was precharged in the bottom of the reactor. The pressure of CO_2 and the temperature of reactor were 0.2 MPa and 323 K, respectively, which were the same as in the solid−gas interface reactions mode. The photocatalytic reaction was typically performed for 10 h. The amounts of CO, CH_4, and H_2 formed were analyzed by gas chromatography (GC). The reaction system was connected to an online GC through valves, and the gaseous products could be directly introduced to the GC for analysis. We adopted a flame ionization detector (FID) for quantifying the amounts of CO and CH_4 formed from CO_2 to ensure high sensitivities. After the effluents containing CO_2, CO, and CH_4 were separated by a carbon molecular sieve (TDX-01) column, CO and CO_2 were further converted to CH_4 by a methanation reactor, and were then analyzed by the FID detector. The detection limits of our analytic method for CH_4 and CO were both 0.002 μmol, corresponding to ~0.5 ppm in concentration. H_2 and O_2 were analyzed by an Agilent Micro GC3000 (Micro GC) equipped with a Molecular Sieve 5A column and a high-sensitivity thermal conductivity detector (TCD). Argon was used as the carrier gas. The Micro GC was connected directly to the reactor by a stainless-steel tube, and the gaseous products were introduced to the Micro GC by a self-suction type injection pump. The detection limits for H_2 and O_2 were 0.004 μmol (~1 ppm) and 0.2 μmol (~50 ppm), respectively. The relative errors for the products except for O_2 were typically lower than 5%. Liquid products such as CH_3OH, HCHO, and HCOOH possibly formed and dissolved in water were also analyzed carefully by gas chromatography or high-performance liquid chromatography, but no such products were detected under our reaction conditions. We performed the same experiment (including both reaction and analysis) for at least 3 times for each catalyst, and the relative standard deviations for the amounts of H_2, CO, and CH_4 formed were <5%.

3. RESULTS AND DISCUSSION

3.1. Influence of Reaction Mode. We performed a comparative study on photocatalytic reduction of CO_2 with H_2O using solid−gas and solid−liquid interface reaction modes. Over our TiO_2 and 0.5 wt % Pt−TiO_2 catalysts, CO and CH_4 were the only products formed from CO_2 irrespective of the reaction mode. The formation of H_2 due to the reduction of H_2O was also observed. We further observed the formation of O_2. These observations suggest the occurrence of the following reactions over our catalysts:

$$CO_2 + 2H^+ + 2e^- \rightarrow CO + H_2O \quad (1)$$

$$CO_2 + 8H^+ + 8e^- \rightarrow CH_4 + 2H_2O \quad (2)$$

$$2H^+ + 2e^- \rightarrow H_2 \quad (3)$$

$$H_2O + 2h^+ \rightarrow 1/2O_2 + 2H^+ \quad (4)$$

To evaluate the efficiency of photogenerated electrons used for the reduction reactions, we have calculated the rate of electron consumption for the formation of all reductive products with the following equation:

$$R(\text{electron}) = 2r(\text{CO}) + 8r(\text{CH}_4) + 2r(\text{H}_2) \quad (5)$$

where $r(CO)$, $r(CH_4)$, and $r(H_2)$ are the formation rates of CO, CH_4, and H_2, respectively. Furthermore, considering that the reduction of H_2O to H_2 is competitive with the reduction of CO_2 to CO and CH_4, we have evaluated the selectivity for CO_2 reduction on an electron basis using the follow equation:

$$\text{Selectivity for CO}_2\text{ reduction (\%)} = [2r(\text{CO}) + 8r(\text{CH}_4)]/[2r(\text{CO}) + 8r(\text{CH}_4) + 2r(\text{H}_2)] \times 100\% \quad (6)$$

Table 1 shows photocatalytic results obtained for TiO_2 and 0.5 wt % Pt−TiO_2 catalysts using two different reaction modes (i.e., the solid−gas and solid−liquid interface reaction modes). For each catalyst, the rates of electron consumption used for reduction, that is, R(electron), with the two reaction modes were similar. However, the rates of product formations depended strongly on the reaction mode. The formation rates of CH_4 and CO with the solid−gas reaction mode were significantly higher than those with the solid−liquid reaction mode, while the formation rate of H_2 was higher with the latter reaction mode. The selectivity of photogenerated electrons for CO_2 reduction was significantly higher with the solid−gas reaction mode.

We speculate that the lower selectivity for CO_2 reduction in the case of using the solid−liquid interface reaction mode is

Table 1. Influence of Reaction Mode on Photocatalytic Performances of TiO_2 and 0.5 wt % Pt−TiO_2 for Reduction of CO_2 in the Presence of H_2O[a]

reaction mode	photocatalyst	formation rate (μmol g^{-1} h^{-1})			R(electron) (μmol g^{-1} h^{-1})	selectivity for CO_2 reduction (%)
		CO	CH_4	H_2		
solid−gas	TiO_2	1.2	0.38	2.1	10	56
solid−liquid	TiO_2	0.80	0.11	5.3	13	19
solid−gas	Pt−TiO_2	1.1	5.2	33	110	40
solid−liquid	Pt−TiO_2	0.76	1.4	55	123	11

[a]Reaction conditions: catalyst, 0.020 g; CO_2 pressure, 0.2 MPa; H_2O, 4.0 mL; irradiation time, 10 h.

dx.doi.org/10.1021/cs500648p | ACS Catal. 2014, 4, 3644−3653

Table 2. Catalytic Behaviors of TiO_2 Promoted by Noble Metal Cocatalysts for Photocatalytic Reduction of CO_2 in the Presence of H_2O Vapor[a]

photocatalyst[b]	formation rate (μmol g^{-1} h^{-1})			R(electron) (μmol g^{-1} h^{-1})	selectivity for CO_2 reduction (%)	work function[c] (eV)
	CO	CH_4	H_2			
TiO_2	1.2	0.38	2.1	10	56	
Pt−TiO_2	1.1	5.2	33	110	40	5.65
Pd−TiO_2	1.1	4.3	25	85	42	5.12
Rh−TiO_2	0.62	3.5	18	66	45	4.98
Au−TiO_2	1.5	3.1	20	67	41	5.10
Ag−TiO_2	1.7	2.1	16	51	39	4.26

[a]Reaction conditions: catalyst, 0.020 g; CO_2 pressure, 0.2 MPa; H_2O, 4.0 mL; irradiation time, 10 h. [b]The content of cocatalyst is 0.5 wt %. [c]From ref 38.

caused by the predominant covering of the catalyst with H_2O due to the limited solubility of CO_2 in H_2O. This leads to higher formation rate of H_2 but lower ones of CH_4 and CO. In other words, a larger fraction of the photogenerated electrons are used for the reduction of H_2O instead of CO_2. The presence of Pt accelerated the rate of electron consumption for reductive reactions, i.e., R(electron), but these electrons were mainly used for the reduction of H_2O to H_2 in the case of the solid−liquid interface reaction mode. On the other hand, the solid−gas interface reaction mode can allow the exposure of the catalyst surface to CO_2 atmosphere and avoid the predominant formation of H_2. Thus, it becomes clear that the solid−gas interface reaction mode is more suitable for the preferential reduction of CO_2 in the presence of H_2O.

3.2. Effect of Noble Metal Cocatalysts. Table 1 also demonstrates that the loading of Pt as a cocatalyst onto TiO_2 can accelerate the photocatalytic performance for product formation. To gain further insights into the role of cocatalysts, we have investigated in more detail the effect of noble metal cocatalysts on the photocatalytic reduction of CO_2 using the solid−gas interface reaction mode. Table 2 shows that the loading of noble metal cocatalysts including Pt, Pd, Rh, Au, and Ag all enhances the rate of consumption of photogenerated electrons for the reductive reactions, i.e., R(electron). R(electron) increased in the sequence of TiO_2 < Ag−TiO_2 < Rh−TiO_2 < Au−TiO_2 < Pd−TiO_2 < Pt−TiO_2. This trend corresponds well to that for the work function of noble metals, which reflects the electron donating or accepting ability and increases in the order of Ag < Rh < Au < Pd < Pt.[38] Thus, it is reasonable to speculate that the cocatalyst may extract the electrons from TiO_2 and, thus, decrease the probability of recombination of photogenerated electrons and holes.

To confirm the role of cocatalyst, we have performed transient photocurrent response measurements. The result displayed in Figure 2 reveals that the photocurrent increases in the sequence of TiO_2 < Ag−TiO_2 < Rh−TiO_2 < Au−TiO_2 < Pd−TiO_2 < Pt−TiO_2, which is in agreement with that for R(electron). This observation further confirms our idea that the noble metal cocatalyst on TiO_2 functions for the extraction of electrons from TiO_2, contributing to the increase in the efficiency of photogenerated electrons for the formation of reductive products.

Table 2 also reveals that the presence of a noble metal cocatalyst significantly increases the rate of CH_4 formation, whereas the rate of CO formation does not increase significantly and it rather decreases when Rh is used as the cocatalyst. In other words, the product selectivity in the reduction of CO_2 is also dependent on the presence of noble metal cocatalyst. It is known that the control of the product

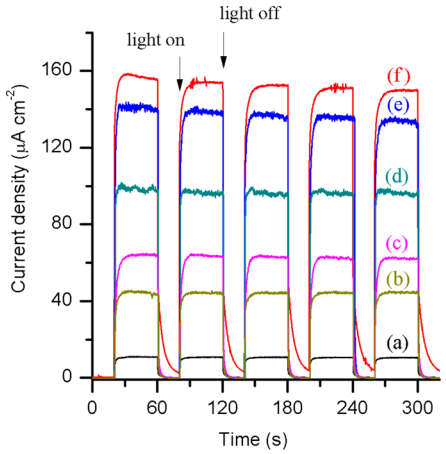

Figure 2. Transient photocurrent responses. (a) TiO_2, (b) Ag/TiO_2, (c) Rh/TiO_2, (d) Au/TiO_2, (e) Pd/TiO_2, (f) Pt/TiO_2.

selectivity during the photocatalytic reduction of CO_2 is challenging, and there is little knowledge on the factors determining the product distribution.[10] Our present work has clearly demonstrated that the selectivity of CH_4 can be markedly enhanced at the expense of CO by loading noble metal cocatalyst onto TiO_2. For example, the Pt−TiO_2 catalyst provided a CH_4 selectivity of 83% on a carbon basis, which was significantly higher than that over TiO_2 (24%). It is reasonable to consider that CO and CH_4 are formed via proton-assisted multielectron transfer reactions [eqs 1 and 2].[39] Thus, the enrichment of electron density on Pt particles may enhance the probability of eight-electron transfer reactions to form CH_4.

The presence of noble metal cocatalyst not only enhanced the reduction of CO_2 to CH_4 but also accelerated the reduction of H_2O to H_2. The selectivity of the photogenerated electrons for CO_2 reduction decreased from 56% for TiO_2 to 39−45% for the catalysts promoted by the noble metals listed in Table 2. In other words, although the use of noble metal cocatalyst can increase the efficiency of electrons used for reductive reactions due to the enhanced electron−hole separation probability, the reduction of H_2O is accelerated more than the reduction of CO_2. It is undoubtedly needed to develop strategies to increase the selectivity of photogenerated electrons for CO_2 reduction.

3.3. Effects of Content and Particle Size of Pt Cocatalyst. It has been clarified that Pt is the most efficient cocatalyst of TiO_2 in promoting the photocatalytic reduction of CO_2 to CH_4. Here, we have performed more detailed studies for the Pt-promoted TiO_2 catalysts. In addition to the photodeposition, we have employed two other methods to prepare the Pt-promoted TiO_2 catalysts. TEM measurements

dx.doi.org/10.1021/cs500648p | ACS Catal. 2014, 4, 3644−3653

showed that the catalyst prepared by the impregnation followed by H_2 reduction (denoted as Pt−TiO_2−*imp*−H_2) possessed larger Pt particles, while the hydrazine reduction provided a catalyst (denoted as Pt−TiO_2−*hydrazine*) with smaller Pt particles (Figure 3). The mean sizes of Pt particles evaluated by

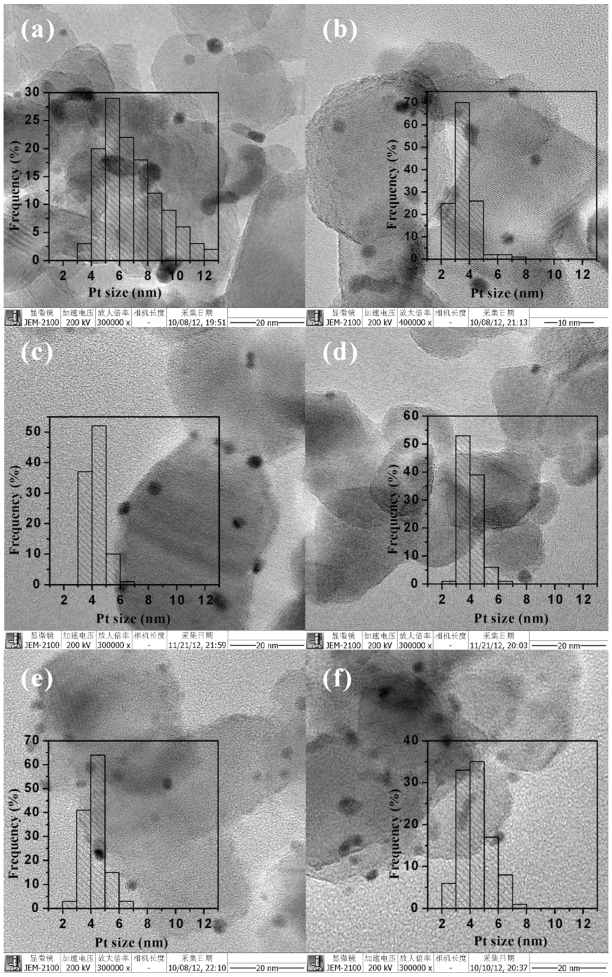

Figure 3. TEM micrographs and the corresponding Pt particle size distributions. (a) 0.5 wt % Pt−TiO_2−*imp*−H_2, (b) 0.5 wt % Pt−TiO_2−*hydrazine*, (c) 0.5 wt % Pt−TiO_2, (d) 0.1 wt % Pt−TiO_2, (e) 1.0 wt % Pt−TiO_2, (f) 2.0 wt % Pt−TiO_2.

counting ∼100 particles were 6.8 and 3.7 nm for these two catalysts, and the latter one was similar to that evaluated for the catalyst prepared by the photodeposition method (denoted as Pt−TiO_2). We further prepared the Pt−TiO_2 catalysts with different Pt loadings, and our TEM measurements clarified that the mean size of Pt particles increased slightly with Pt loadings (Figure 3).

Table 3 displays the catalytic behaviors of the Pt-promoted TiO_2 catalysts prepared by different methods as well as the Pt−TiO_2 catalysts with different Pt loadings for photocatalytic reduction of CO_2. It is clear that the loading of Pt can significantly enhance the formation of CH_4, but the reduction of H_2O to H_2 is also accelerated at the same time. We found that the photocatalytic behavior is dependent on the mean size of Pt particles. Among the 0.5 wt % Pt-promoted TiO_2 catalysts prepared by different methods, the 0.5 wt % Pt−TiO_2−*imp*−H_2 catalyst with the largest mean size of Pt particles exhibited the lowest CH_4 formation activity. The formation of CO was slightly enhanced, and the selectivity of CH_4 in CO_2 reduction products was the lowest (40% on carbon basis) over this catalyst. On the other hand, the 0.5 wt % Pt−TiO_2−*hydrazine* and 0.5 wt % Pt−TiO_2, which possessed Pt particles with similar mean sizes, showed similar photocatalytic performances. The rates of CH_4 formations were 5.0 and 5.2 μmol g^{-1} h^{-1} over these two catalysts, which were ∼13 and ∼4 times higher than those over TiO_2 and the 0.5 wt % Pt−TiO_2−*imp*−H_2, respectively.

Further analysis revealed that the rates of consumption of photogenerated electrons for reductive reactions described by *R*(electron) over the 0.5 wt % Pt−TiO_2−*hydrazine* and 0.5 wt % Pt−TiO_2 catalysts were 1 order of magnitude and ∼2.5 times higher than those over TiO_2 and the 0.5 wt % Pt−TiO_2−*imp*−H_2 catalysts, respectively. This suggests the difference in the separation of photogenerated electron and hole pairs among the Pt-promoted catalysts prepared by different methods. We have exploited the photoluminescence (PL) spectroscopy, which is a powerful tool to provide information on surface processes involving the recombination of photogenerated charge carriers,[40] for our 0.5 wt % Pt-promoted TiO_2 catalysts prepared by different methods. Generally, the photoluminescence can be generated during the recombination of the photogenerated carriers on a semiconductor. We observed a visible luminescence band centered at ∼500 nm for TiO_2 (Figure 4A). This could be ascribed to the recombination of photoexcited electrons and holes possibly due to the oxygen vacancies on TiO_2.[40] When Pt was loaded onto TiO_2, the intensity of the luminescence band at ∼500 nm decreased, suggesting a reduced charge carrier recombination. This can be explained by the migration of excited electrons from TiO_2 to the Pt nanoparticle, preventing the electron−hole recombination. Our result in Figure 4 suggests that the smaller Pt

Table 3. Catalytic Behaviors of Pt−TiO_2 Catalysts Prepared by Different Methods or with Different Pt Loadings for Photocatalytic Reduction of CO_2 in the Presence of H_2O Vapor[a]

photocatalyst	Pt particle size (nm)	formation rate (μmol g^{-1} h^{-1})			*R*(electron) (μmol g^{-1} h^{-1})	selectivity for CO_2 reduction (%)
		CO	CH_4	H_2		
TiO_2		1.2	0.38	2.1	10	56
0.5% Pt−TiO_2−*imp*−H_2	6.8	1.8	1.2	14	41	33
0.5% Pt−TiO_2−*hydrazine*	3.7	0.62	5.0	28	97	42
0.5% Pt−TiO_2	4.2	1.1	5.2	33	110	40
0.1% Pt−TiO_2	4.0	1.0	1.5	11	36	38
1.0% Pt−TiO_2	4.3	0.54	6.1	36	122	41
2.0% Pt−TiO_2	4.4	0.59	4.3	26	89	41

[a]Reaction conditions: catalyst, 0.020 g; CO_2 pressure, 0.2 MPa; H_2O, 4.0 mL; irradiation time, 10 h.

dx.doi.org/10.1021/cs500648p | *ACS Catal.* 2014, 4, 3644−3653

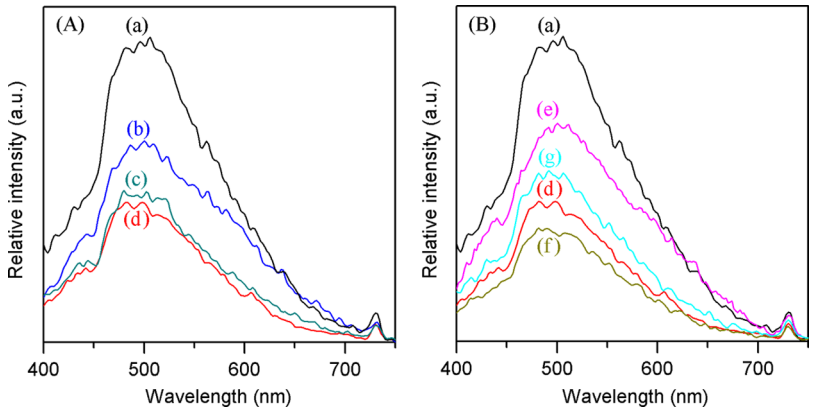

Figure 4. Photoluminescence spectra. (A) 0.5 wt % Pt−TiO_2 prepared by different methods and TiO_2: (a) TiO_2, (b) 0.5 wt % Pt−TiO_2−*imp*−H_2, (c) 0.5 wt % Pt−TiO_2−*hydrazine*, (d) 0.5 wt % Pt−TiO_2. (B) Pt−TiO_2 prepared by photodeposition with different Pt loadings: (d) 0.5 wt % Pt−TiO_2, (e) 0.1 wt % Pt−TiO_2, (f) 1.0 wt % Pt−TiO_2, (g) 2.0 wt % Pt−TiO_2.

nanoparticles over the 0.5 wt % Pt−TiO_2−*hydrazine* and 0.5 wt % Pt−TiO_2 catalysts are more efficient to extract the electrons from TiO_2 than the bigger ones over the 0.5 wt % Pt−TiO_2−*imp*−H_2 due to the larger interfaces between Pt and TiO_2 in the former two catalysts. This corresponds well to the higher rates of consumption of photogenerated electrons for reductive reactions over the 0.5 wt % Pt−TiO_2−*hydrazine* and 0.5 wt % Pt−TiO_2 catalysts.

Concerning the selectivity of photogenerated electrons for CO_2 reduction, the value was lower over the 0.5 wt % Pt−TiO_2−*imp*−H_2 catalyst than those over the 0.5 wt % Pt−TiO_2−*hydrazine* and 0.5 wt % Pt−TiO_2 catalysts. Thus, the catalyst with larger Pt particles accelerated the reduction of H_2O to H_2 more than the reduction of CO_2. Possibly, H_2O was preferentially chemisorbed on the surfaces of larger Pt particles. Moreover, our result showed that the catalyst with bigger Pt particles exhibited lower selectivity to CH_4 in CO_2 reduction products as compared to those with smaller Pt particles. This is likely due to the relatively lower electron density on bigger Pt particles.

The photocatalytic result for the Pt−TiO_2 catalysts with different Pt loadings showed that the increase in the Pt loading from 0.1 wt % to 1.0 wt % increased both CH_4 and H_2 formation rates (Table 3). CO formation rate rather decreased at a Pt loading of 1.0 wt %. The selectivity of photogenerated electrons for CO_2 reduction changed only slightly with Pt loading. The rate of electron consumption for reduction reactions, i.e., R(electron), increased with Pt loadings up to 1.0 wt %. A further increase in the Pt loading to 2.0 wt % decreased R(electron) and also the rates of CH_4 and H_2 formations. The PL spectra for this series of catalysts revealed that the increase in the Pt loading up to 1.0 wt % decreased the intensity of the luminescence band at ∼500 nm, and thus, the probability of charge carrier recombination. The intensity of the luminescence band at ∼500 nm increased as the Pt loading rose to 2.0 wt % (Figure 4B), suggesting that the excessively high Pt loading is rather unfavorable for the separation of electron−hole pair. It is speculated that the electron generated on TiO_2 can be extracted to a Pt particle nearby and the distance between the hole remaining on TiO_2 and the Pt particle may become shorter if the Pt loading becomes higher.[41] This may increase the probability of recombination of electrons and holes. This result corresponds well to the decreases in R(electron) and the formation rates of CH_4 and H_2 at the higher Pt loading (2.0 wt %).

3.4. Effect of MgO on Catalytic Behaviors of Pt−TiO_2.

A few papers have demonstrated that the addition of MgO can promote photocatalytic performances of TiO_2-based catalysts for CO_2 reduction possibly due to the enhancement in CO_2 chemisorption or the generated Ti^{3+} sites.[42−44] However, it is still unclear whether the presence of MgO can accelerate the separation of electron−hole pairs. Moreover, there is no information on the effect of MgO on the selectivity of photogenerated electrons for CO_2 reduction.

To clarify the roles of MgO in photocatalytic reduction of CO_2, we have prepared MgO−Pt−TiO_2 catalysts with MgO contents ranging from 0.25 to 3.0 wt %. TEM measurements clarified that MgO existed as amorphous layers on TiO_2 (Figure 5). The mean size of Pt evaluated from the TEM micrographs by counting ∼100 particles was almost independent of MgO

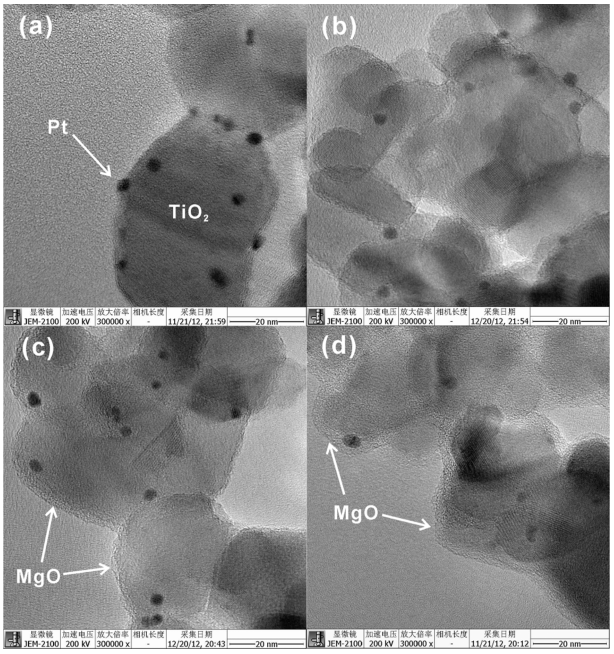

Figure 5. TEM micrographs. (a) 0.5 wt % Pt−TiO_2, (b) 0.25 wt % MgO−0.5 wt % Pt−TiO_2, (c) 1.0 wt % MgO−0.5 wt % Pt−TiO_2, (d) 3.0 wt % MgO−0.5 wt % Pt−TiO_2.

dx.doi.org/10.1021/cs500648p | *ACS Catal.* 2014, 4, 3644−3653

Table 4. Effect of MgO on Catalytic Behaviors of Pt−TiO_2 for Photocatalytic Reduction of CO_2 in the Presence of H_2O Vapor[a]

photocatalyst[b]	CO_2 chemisorbed (μmol g^{-1})	formation rate (μmol g^{-1} h^{-1})			R(electron) (μmol g^{-1} h^{-1})	selectivity for CO_2 reduction (%)
		CO	CH_4	H_2		
TiO_2	5.0	1.2	0.38	2.1	10	56
Pt−TiO_2	5.1	1.1	5.2	33	110	40
0.25% MgO−Pt−TiO_2	7.4	0.29	6.5	29	111	47
0.5% MgO−Pt−TiO_2	10	0.03	8.1	23	111	59
1.0% MgO−Pt−TiO_2	12	0.03	11	11	110	79
2.0% MgO−Pt−TiO_2	15	0.03	8.9	8.4	88	81
3.0% MgO−Pt−TiO_2	17	0.02	6.3	5.1	61	83

[a]Reaction conditions: catalyst, 0.020 g; CO_2 pressure, 0.2 MPa; H_2O, 4.0 mL; irradiation time, 10 h. [b]The loading of Pt was 0.5 wt %.

content. We also measured the amount of CO_2 chemisorption over this series of catalysts and found that the amount of CO_2 chemisorption increased with MgO content (Table 4).

Our photocatalytic result in Table 4 showed that the rate of consumption of photogenerated electrons for reductive reactions, i.e., R(electron), did not change significantly by the addition of MgO into the Pt−TiO_2 catalyst with contents of 0−1.0 wt %. The further addition of MgO rather decreased R(electron). Our transient photocurrent response measurements clarified that the photocurrent decreased slightly after the addition of MgO to the Pt−TiO_2 catalyst with contents of 0−1.0 wt % (Figure 6). The decrease in the photocurrent

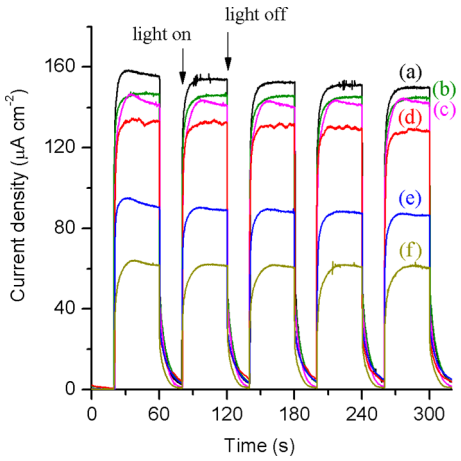

Figure 6. Transient photocurrent responses. (a) 0.5 wt % Pt−TiO_2, (b) 0.25 wt % MgO−0.5 wt % Pt−TiO_2, (c) 0.5 wt % MgO−0.5 wt % Pt−TiO_2, (d) 1.0 wt % MgO−0.5 wt % Pt−TiO_2, (e) 2.0 wt % MgO−0.5 wt % Pt−TiO_2, (f) 3.0 wt % MgO−0.5 wt % Pt−TiO_2.

became significant when the content of MgO was ≥2.0 wt %. This clearly suggests that the ability to separate the electron−hole pairs does not change significantly by the addition of MgO with a content of 0.25−1.0 wt %. The larger amount of MgO decreased R(electron), probably because the excess MgO may significantly cover TiO_2 surface and/or hinder the migration of photogenerated electrons from TiO_2 to Pt particles.

It is of interest that, although R(electron) did not increase by the addition of MgO to the Pt−TiO_2 catalyst, the rate of CH_4 formation increased significantly from 5.2 to 11 μmol g^{-1} h^{-1} as the content of MgO rose from 0 to 1.0 wt %. At the same time, the rate of CO formation decreased from 1.1 to 0.03 μmol g^{-1} h^{-1}. Thus, the selectivity of CH_4 in CO_2 reduction products increased to >99% (on carbon basis). The rate of H_2 formation decreased from 33 to 11 μmol g^{-1} h^{-1} on increasing the content of MgO from 0 to 1.0 wt %. Therefore, the selectivity of photogenerated electrons for CO_2 reduction increased markedly from 40 to 79%. A further increase in MgO content did not change the selectivity significantly, but the rates of product formations decreased due to the covering of TiO_2 by MgO or the hindering of electron transfer between TiO_2 and Pt as evidenced by the significant decrease in the photocurrent at higher MgO contents (≥2.0 wt %, Figure 6).

Figure 7 shows the changes of product amounts with the reaction time during the photocatalytic reduction of CO_2 over

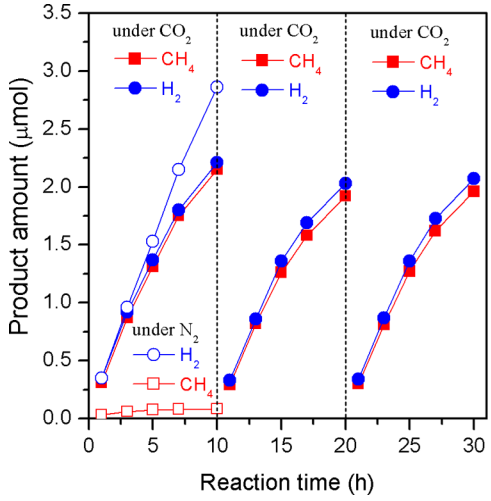

Figure 7. Changes of product amounts with reaction time and repeated uses of the 1.0 wt % MgO−0.5 wt % Pt−TiO_2 catalyst for photocatalytic reduction of CO_2 in the presence of H_2O vapor. Reaction conditions: catalyst, 0.020 g; CO_2 pressure, 0.2 MPa; H_2O, 4 mL. After each 10 h, the system was degassed, and then CO_2 was reintroduced into the reactor.

the 1.0 wt % MgO−0.5 wt % Pt−TiO_2 catalyst. The amounts of CH_4 and H_2 both increased almost linearly with the reaction time. Bazzo and Urakawa recently reported transient formations of H_2 and CH_4 in initial 1 h followed by rapid deactivation during the photocatalytic reduction of CO_2 at relatively higher temperatures (353 and 423 K) over a Pt/TiO_2 catalyst.[45] The almost linear increases in the product amounts with time in Figure 7 allow us to confirm that the formations of both CH_4 and H_2 over our catalyst proceed in a steady-state manner but not a transient manner. We performed the repeated uses of the 1.0 wt % MgO−0.5 wt % Pt−TiO_2 catalyst. After 10 h, the system was degassed and then CO_2 was reintroduced into the reactor (Figure 7). Similar activities for the formations of CH_4 and H_2 were observed in the second and the third runs.

dx.doi.org/10.1021/cs500648p | ACS Catal. 2014, 4, 3644−3653

Table 5. Catalytic Behaviors of $Pt-TiO_2$ and $MgO-Pt-TiO_2$ in Several Control Experiments[a]

photocatalyst[b]	reaction atmosphere	irradiation	formation rate (μmol g^{-1} h^{-1})		
			CO	CH_4	H_2
$Pt-TiO_2$	$CO_2 + H_2O$ vapor	yes	1.1	5.2	33
$Pt-TiO_2$	$CO + H_2O$ vapor	yes		3.2	68
$Pt-TiO_2$	$H_2 + CO_2$[c]	no	0	0	
$Pt-TiO_2$	$H_2 + CO$[c]	no		0	
$MgO-Pt-TiO_2$	$CO_2 + H_2O$ vapor	yes	0.03	11	11
$MgO-Pt-TiO_2$	$CO + H_2O$ vapor	yes		5.2	92
$MgO-Pt-TiO_2$	$H_2 + CO_2$[c]	no	0	0	
$MgO-Pt-TiO_2$	$H_2 + CO$[c]	no		0	

[a]Reaction conditions: catalyst, 0.020 g; pressure, 0.2 MPa; H_2O, 4.0 mL; time, 10 h. [b]The loading of Pt was 0.5 wt %; the content of MgO was 1.0 wt %. [c]H_2/CO_2 or H_2/CO = 1/99.

This suggests that the reactions over our photocatalyst are catalytic reactions but not stoichiometric ones. Our result in Figure 7 also indicates that the 1.0 wt % MgO−0.5 wt % $Pt-TiO_2$ catalyst is stable under our reaction conditions. We further carried out the photocatalytic reaction in the absence of CO_2. As displayed in Figure 7, when N_2 was used instead of CO_2 over the 1.0 wt % MgO−0.5 wt % $Pt-TiO_2$ catalyst, H_2 was formed and the amount of H_2 was slightly larger than that formed in the presence of CO_2. However, no CO and only a trace amount of CH_4 were detected in the absence of CO_2 (<0.1 μmol in 10 h). This confirms that CH_4 is formed predominantly via the photocatalytic reduction of CO_2 over our catalyst.

The amount of O_2 formed during the photocatalytic reduction of CO_2 in the presence of H_2O was also quantified for several catalysts, although the experimental error for O_2 quantification was larger than that for H_2, CO or CH_4 quantification. For example, for the 1.0 wt % MgO−0.5 wt % $Pt-TiO_2$ catalyst, the amount of O_2 detected was 13.6 μmol after 30 h of reaction under typical reaction conditions (catalyst, 0.020 g; CO_2 pressure, 0.2 MPa; H_2O, 4 mL). At the same time, the amounts of H_2 and CH_4 formed were 6.3 and 5.5 μmol, respectively. Only a trace amount of CO was detected. If we assume that the oxidation of H_2O to O_2 is the sole reaction to consume the photogenerated holes [eq 4] and that the photogenerated electrons are used for the formations of CO, CH_4, and H_2 [eqs 1−3], the stoichiometric molar ratio of $O_2/(CO + 4CH_4 + H_2)$ should be 1/2. The molar ratio of $O_2/(CO + 4CH_4 + H_2)$ calculated from our results was 0.48, which was close to the stoichiometric ratio. This suggests that the reactions of eqs 1−4 mainly occur over our photocatalysts and also provides evidence that CH_4 is formed from the photocatalytic reduction of CO_2.

Therefore, it becomes clear that the $MgO-Pt-TiO_2$ catalyst with a proper MgO content (1.0 wt %) is a highly selective catalyst for the preferential reduction of CO_2 in the presence of H_2O. Moreover, CH_4 is the predominant product in the reduction of CO_2 over this photocatalyst. We have demonstrated that MgO plays a key role in enhancing the preferential photocatalytic reduction of CO_2 to CH_4 in the presence of H_2O. Tanaka and co-workers reported that MgO or MgO-containing layered double hydroxides could work for the photocatalytic reduction of CO_2 to CO in the presence of H_2 or H_2O.[46] However, MgO or Pt-loaded MgO without TiO_2 was inactive for the photocatalytic conversion of CO_2 with H_2O under our reaction conditions. Thus, MgO should function as a cocatalyst of TiO_2 together with Pt in our system. Although it has been clarified that MgO cannot increase the ability to separate the electron−hole pairs, the presence of MgO significantly increases the chemisorption of CO_2. On the basis of these results, we propose that MgO provides basic sites for the preferential chemisorption of CO_2 onto the catalyst surface and these chemisorbed CO_2 molecules can be efficiently reduced by the electrons on the nearby Pt nanoparticles extracted from TiO_2.

3.5. Discussion on Possible Reaction Mechanism. As mentioned previously, the control of selectivity, including both the selectivity of photogenerated electrons for CO_2 reduction and the selectivity of products in CO_2 reduction, is a challenging research target.[10] Our present work has demonstrated that the modification of TiO_2 with Pt and MgO can significantly promote the selectivity of photogenerated electrons for CO_2 reduction and for CH_4 formation. To gain insights into the pathways for CO and CH_4 formations over our photocatalysts would be helpful to understand the promoting effects in depth.

Generally, it is difficult to consider the successive single-electron transfer mechanism for the formations of CO and CH_4 because the potential for the single-electron reduction of CO_2 (−2.14 V vs SCE) is highly unfavorable.[39] Instead, the reduction of CO_2 can be expected to proceed via the proton-assisted multielectron transfer mechanism. However, the reduction of CO_2, in particular the formation of CH_4, is quite complicated. CH_4 may be produced via the direct reduction of CO_2 through eight-electron mechansim [eq 2], via the hydrogenation of CO_2 under dark by the hydrogen formed via the photocatalytic reduction of H_2O [eq 7], or via CO through the hydrogenation under dark or irradiation [eqs 8 and 9].[28,29]

$$CO_2 + 4H_2 \rightarrow CH_4 + 2H_2O \quad (7)$$

$$CO + 3H_2 \rightarrow CH_4 + H_2O \quad (8)$$

$$CO + 6H^+ + 6e^- \rightarrow CH_4 + H_2O \quad (9)$$

To gain information on the pathway for CH_4 formation, we have performed several control experiments. Table 5 shows that the hydrogenation of CO_2 or CO over our catalysts, including both $Pt-TiO_2$ and $MgO-Pt-TiO_2$, cannot proceed under dark reaction conditions. This rules out the possibility that CH_4 is formed via the hydrogenation of CO_2 or CO under dark conditions by the hydrogen resulting from the photocatalytic reduction of H_2O [eqs 7 and 8]. The use of CO as a reactant instead of CO_2 under irradiation conditions could take place, producing CH_4 and H_2. This suggests that the photocatalytic reduction of CO in the presence of H_2O, i.e., reaction 9, can

dx.doi.org/10.1021/cs500648p | ACS Catal. 2014, 4, 3644−3653

take place over our catalysts. However, it should be noted that the rate of CH_4 formation in the photocatalytic reduction of CO is significantly lower than that in the photocatalytic reduction of CO_2, although CO_2 is believed to be more difficult to activate. On the other hand, the rate of H_2 formation, which arose from the photocatalytic reduction of H_2O, became significantly higher when CO was used to replace CO_2. These observations clearly demonstrate that our photocatalysts are more efficient for the photocatalytic reduction of CO_2 than that of CO. On the basis of these experimental results, we propose that CH_4 is mainly formed via the direct photocatalytic reduction of CO_2, although we cannot completely rule out the possibility that a part of CH_4 may be formed via the photocatalytic reduction of CO.

It can be expected that the formations of CH_4 and CO, two parallel products, are the compromise between the thermodynamics and the charge transfer.[29] On the one hand, the formation of CH_4 is thermodynamically more favorable than that of CO.[39] On the other hand, the formation of CH_4 requires eight electrons, while that of CO only needs two electrons. CO was formed as a major product over TiO_2 possibly because of the low density of electrons. It can be easily understood that the loading of Pt increases the selectivity of CH_4 because the enrichment of electron density on Pt particles can enhance the probability of multielectron reactions to CH_4. One of the most significant points of our present work is the further increase in CH_4 selectivity by the addition of MgO, although the electron density on Pt is not further accelerated as evidenced by the photocurrent measurements. At the same time, the selectivity of photogenerated electrons used for CO_2 reduction as compared to those for H_2O reduction also increases in the presence of MgO. The enhanced chemisorption of CO_2 on catalyst surfaces due to the presence of MgO could accelerate the reduction of CO_2 and suppress that of H_2O. Furthermore, we speculate that the synergistic effect between MgO and Pt, which enhanced the chemisorption of CO_2 and the electron density, is responsible for the selective formation of CH_4.

4. CONCLUSIONS

The present work focused on the development of efficient photocatalytic systems for the preferential photocatalytic reduction of CO_2 in the presence of H_2O. We found that the use of the solid−gas interface reaction mode, i.e., the reaction of CO_2 with H_2O vapor, resulted in higher selectivity of photogenerated electrons toward the reduction of CO_2 to CO and CH_4 as compared to the reduction of H_2O to H_2. The predominant exposure of catalyst surface to H_2O, which was the case in the solid−liquid interface reactions, could be avoided in the solid−gas interface reactions. We studied the effect of cocatalysts on catalytic behaviors of TiO_2 for photocatalytic reduction of CO_2 using the solid−gas interface reaction mode. Among several noble metals including Pt, Pd, Rh, Au, and Ag, Pt was the most efficient cocatalyst to extract the photogenerated electrons for the reductive reactions. The loading of Pt onto TiO_2 also increased the selectivity of CH_4 and decreased that of CO possibly because the enhanced electron density favored the eight-electron reduction of CO_2 to CH_4. The size and loading amount of Pt also affected the photocatalytic behavior of Pt−TiO_2 catalysts. The catalysts with smaller Pt particles and proper Pt loadings favored the CH_4 formation rate and CH_4 selectivity. However, the presence of Pt also accelerated the reduction of H_2O to H_2, and the selectivity of photogenerated electrons for CO_2 reduction rather decreased slightly. We demonstrated that the addition of MgO to the Pt−TiO_2 catalyst significantly increased the selectivity for CO_2 reduction although the rate of electron consumption for reductive reactions did not change significantly. The presence of MgO remarkably suppressed the reduction of H_2O to H_2 and accelerated the reduction of CO_2. Furthermore, the addition of MgO into the Pt−TiO_2 catalyst further improved the selectivity of CH_4 in CO_2 reduction to >99%. The synergistic effect between the enhanced CO_2 chemisorption and electron density on the surface of MgO- and Pt-co-promoted TiO_2 is proposed to be responsible for the improvement of the selectivity for CO_2 reduction and CH_4 formation. Our work has provided important clues for selectivity control in the photocatalytic reduction of CO_2 in the presence of H_2O.

AUTHOR INFORMATION

Corresponding Authors

*E-mail: wangye@xmu.edu.cn. Fax: +86-592-2183047. Tel.: +86-592-2186156.

*E-mail: zhanqh@xmu.edu.cn.

Notes

The authors declare no competing financial interest.

ACKNOWLEDGMENTS

This work was supported by the Natural Science Foundation of China (Nos. 21173172, 21033006, and 21161130522), the National Basic Research Program of China (No. 2013CB933100), the Research Fund for the Doctoral Program of Higher Education (2013012113001), and the Program for Innovative Research Team in Chinese Universities (No. IRT1036).

REFERENCES

(1) For recent reviews on catalytic transformations of CO_2, see the following: (a) Song, C. S. *Catal. Today* **2006**, *115*, 2−32. (b) Sakakura, T.; Choi, J. C.; Yasuda, H. *Chem. Rev.* **2007**, *107*, 2365−2387. (c) Centi, G.; Perathoner, S. *Catal. Today* **2009**, *148*, 191−205. (d) Mikkelsen, M.; Jørgensen, M.; Krebs, F. C. *Energy Environ. Sci.* **2010**, *3*, 43−81. (e) Hunt, A. J.; Sin, E. H. K.; Marriott, R.; Clark, J. H. *ChemSusChem* **2010**, *3*, 306−322. (f) Wang, W.; Wang, S.; Ma, X.; Gong, J. *Chem. Soc. Rev.* **2011**, *40*, 3703−3727. (g) Wang, Q.; Luo, J.; Zhong, Z.; Borgna, A. *Energy Environ. Sci.* **2011**, *4*, 42−55. (h) Goeppert, A.; Czaun, M.; Prakash, G. K. S.; Olah, G. A. *Energy Environ. Sci.* **2012**, *5*, 7833−7853. (i) Perathoner, S.; Centi, G. *ChemSusChem* **2014**, *7*, 1274−1282.

(2) Inoue, T.; Fujishima, A.; Konishi, S.; Honda, K. *Nature* **1979**, *277*, 637−638.

(3) Indrakanti, V. P.; Kubicki, J. D.; Schobert, H. H. *Energy Environ. Sci.* **2009**, *2*, 745−758.

(4) Roy, S. C.; Varghese, O. K.; Paulose, M.; Grimes, C. A. *ACS Nano* **2010**, *4*, 1259−1278.

(5) Dhakshinamoorthy, A.; Navalon, S.; Corma, A.; Garcia, H. *Energy Environ. Sci.* **2012**, *5*, 9217−9233.

(6) Mori, K.; Yamashita, H.; Anpo, M. *RSC Adv.* **2012**, *2*, 3165−3172.

(7) Fan, W.; Zhang, Q.; Wang, Y. *Phys. Chem. Chem. Phys.* **2013**, *15*, 2632−2649.

(8) Mao, J.; Li, K.; Peng, Y. *Catal. Sci. Technol.* **2013**, *3*, 2481−2498.

(9) Habisreutinger, S. N.; Schmidt-Mende, L.; Stolarczyk, J. K. *Angew. Chem., Int. Ed.* **2013**, *52*, 7372−7408.

(10) Corma, A.; Garcia, H. *J. Catal.* **2013**, *308*, 168−175.

(11) Yang, M. Q.; Xu, Y. J. *Phys. Chem. Chem. Phys.* **2013**, *15*, 19102−19118.

(12) Li, K.; An, X.; Park, K. H.; Khraisheh, M.; Tang, J. *Catal. Today* **2014**, *224*, 3−12.
(13) Tu, W.; Zhou, Y.; Zou, Z. *Adv. Mater.* **2014**, *26*, 4607−4626.
(14) (a) Liu, L.; Zhao, H.; Andino, J. M.; Li, Y. *ACS Catal.* **2012**, *2*, 1817−1828. (b) Zhao, H.; Liu, L.; Andino, J. M.; Li, Y. *J. Mater. Chem. A* **2013**, *1*, 8209−8216.
(15) Jiao, W.; Wang, L.; Liu, G.; Lu, G. Q.; Cheng, H. M. *ACS Catal.* **2012**, *2*, 1854−1859.
(16) Park, H.; Choi, J. H.; Choi, K. M.; Lee, D. K.; Kang, J. K. *J. Mater. Chem.* **2012**, *22*, 5304−5307.
(17) Tsuneoka, H.; Teramura, K.; Shishido, T.; Tanaka, T. *J. Phys. Chem. C* **2010**, *114*, 8892−8898.
(18) (a) Liu, Q.; Zhou, Y.; Kou, J.; Chen, X.; Tian, Z.; Gao, J.; Yan, S.; Zou, Z. *J. Am. Chem. Soc.* **2010**, *132*, 14385−14387. (b) Yan, S.; Wan, L.; Li, Z.; Zou, Z. *Chem. Commun.* **2011**, *47*, 5632−5634. (c) Liu, Q.; Zhou, Y.; Tian, Z.; Chen, X.; Gao, J.; Zou, Z. *J. Mater. Chem.* **2012**, *22*, 2033−2038.
(19) Zhang, N.; Ouyang, S.; Li, P.; Zhang, Y.; Xi, G.; Kako, T.; Ye, J. *Chem. Commun.* **2011**, *47*, 2041−2043.
(20) (a) Yan, S. C.; Ouyang, S. X.; Gao, J.; Yang, M.; Feng, J. Y.; Fan, X. X.; Wan, L. J.; Li, Z. S.; Ye, J.; Zhou, Y.; Zou, Z. *Angew. Chem., Int. Ed.* **2010**, *49*, 6400−6404. (b) Yan, S.; Yu, H.; Wang, N.; Li, Z.; Zou, Z. *Chem. Commun.* **2012**, *48*, 1048−1050. (c) Yan, S.; Wang, J.; Gao, H.; Wang, N.; Yu, H.; Li, Z.; Zhou, Y.; Zou, Z. *Adv. Funct. Mater.* **2013**, *23*, 758−763.
(21) Zhang, N.; Ouyang, S.; Kako, T.; Ye, J. *Chem. Commun.* **2012**, *48*, 1269−1271.
(22) Iizuka, K.; Wato, T.; Miseki, Y.; Saito, K.; Kudo, A. *J. Am. Chem. Soc.* **2011**, *133*, 20863−20868.
(23) Xi, G.; Ouyang, S.; Li, P.; Ye, J.; Ma, Q.; Su, N.; Bai, H.; Wang, C. *Angew. Chem., Int. Ed.* **2012**, *51*, 2395−2399.
(24) Chen, X.; Zhou, Y.; Li, Q.; Li, Z.; Liu, J.; Zou, Z. *ACS Appl. Mater. Interfaces* **2012**, *4*, 3372−3377.
(25) Zhou, Y.; Tian, Z.; Zhao, Z.; Liu, Q.; Kou, J.; Chen, X.; Gao, J.; Yan, S.; Zou, Z. *ACS Appl. Mater. Interfaces* **2011**, *3*, 3594−3601.
(26) Cheng, H.; Huang, B.; Liu, Y.; Wang, Z.; Qin, X.; Zhang, X.; Dai, Y. *Chem. Commun.* **2012**, *48*, 9729−9731.
(27) Zhang, N.; Cirimnna, R.; Pagliaro, M.; Xu, Y. J. *Chem. Soc. Rev.* **2014**, *43*, 5276−5287.
(28) Varghese, O. K.; Paulose, M.; LaTempa, T. J.; Grimes, G. A. *Nano Lett.* **2009**, *9*, 731−737.
(29) Wang, W.; An, W.; Ramalingam, B.; Mukherjee, S.; Niedzwiedzki, D. M.; Gangopadhyay, S.; Biswas, P. *J. Am. Chem. Soc.* **2012**, *134*, 11276−11281.
(30) (a) Wang, C.; Thompson, R. L.; Baltrus, J.; Matranga, C. *J. Phys. Chem. Lett.* **2010**, *1*, 48−53. (b) Wang, C.; Thompson, R. L.; Ohodnicki, P.; Baltrus, J.; Matranga, C. *J. Mater. Chem.* **2011**, *21*, 13452−13457.
(31) Wang, W.; Park, J.; Biswas, P. *Catal. Sci. Technol.* **2011**, *1*, 593−600.
(32) Zhang, X.; Han, F.; Shi, B.; Farsinezhad, S.; Dechaine, G. P.; Shankar, K. *Angew. Chem., Int. Ed.* **2012**, *51*, 12732−12735.
(33) In, S. I.; Vaughn, D. D.; Schaak, R. E. *Angew. Chem., Int. Ed.* **2012**, *51*, 3915−3918.
(34) Zhao, C.; Liu, L.; Zhang, Q.; Wang, J.; Li, Y. *Catal. Sci. Technol.* **2012**, *2*, 2558−2568.
(35) Zhai, Q.; Xie, S.; Fan, W.; Zhang, Q.; Wang, Y.; Deng, W.; Wang, Y. *Angew. Chem., Int. Ed.* **2013**, *52*, 5776−5779.
(36) Teramura, K.; Okuoka, S.; Tsuneoka, H.; Shishido, T.; Tanaka, T. *Appl. Catal., B* **2010**, *96*, 565−568.
(37) Ye, A.; Fan, W.; Zhang, Q.; Deng, W.; Wang, Y. *Catal. Sci. Technol.* **2012**, *2*, 969−978.
(38) Michaelson, H. B. *J. Appl. Phys.* **1977**, *48*, 4729−4733.
(39) Morris, A. J.; Meyer, G. J.; Fujita, E. *Acc. Chem. Res.* **2009**, *42*, 1983−1994.
(40) Shi, J.; Chen, J.; Feng, Z.; Chen, T.; Lian, Y.; Wang, X.; Li, C. *J. Phys. Chem. C* **2007**, *111*, 693−699.
(41) Sadeghi, M.; Liu, W.; Zhang, T. G.; Stavropoulos, P.; Levy, B. *J. Phys. Chem.* **1996**, *100*, 19466−19474.
(42) Xie, S.; Wang, Y.; Zhang, Q.; Fan, W.; Deng, W.; Wang, Y. *Chem. Commun.* **2013**, *49*, 2451−2453.
(43) Liu, L.; Zhao, C.; Zhao, H.; Pitts, D.; Li, Y. *Chem. Commun.* **2013**, *49*, 3664−3666.
(44) Manzanares, M.; Fábrega, C.; Ossó, J. O.; Vega, L. F.; Andreu, T.; Morante, J. R. *Appl. Catal., B* **2014**, *150−151*, 57−62.
(45) Bazzo, A.; Urakawa, A. *ChemSusChem* **2013**, *6*, 2095−2102.
(46) (a) Kohno, Y.; Ishikawa, H.; Tanaka, T.; Funabiki, T.; Yoshida, S. *Phys. Chem. Chem. Phys.* **2001**, *3*, 1108−1113. (b) Teramura, K.; Iguchi, S.; Mizuno, Y.; Shishido, T.; Tanaka, T. *Angew. Chem., Int. Ed.* **2012**, *51*, 8008−8011.